Study of our star, the sun

Sultana N. Nahar

Department of Astronomy, The Ohio State University, Columbus, OH 43210, USA.

Email – nahar.1@osu.edu

Abstract- Our sun is studied extensively as it is the standard for a typical star. However, the knowledge about sun still holds large discrepancies. Recent determination from 3D model of abundances of light elements, such as, carbon, nitrogen, oxygen etc in the sun are up to 30-40% lower than the known standard values from helioseismology. Much of these discrepancies could be reduced if the present value of mean opacity, the fundamental quantity for radiation transport, of the solar plasma is increased by 15%. Opacity is related to abundances since the propagating radiation in plasmas is absorbed and emitted by the constituent elements causing the opacity effect. Sandia National LAB (SNL) which has been increasing the plasma condition to higher temperature and density for opacity experiments has reached the level of creating condition of that in the solar interior at the base of convection zone near radiative zone boundary and has measured the solar opacity. The measured opacity at SNL is found to be 30-400% higher than predictions, such as, that calculated using the Opacity Project atomic data. The integrated mean opacity from the measurement is about 7% higher agreeing with the recent determinations. On the theoretical side, new largescale calculations under the Iron Project and Iron Opacity Project are revealing existence of extensive and dominant resonant features in the high energy photoionization not seen under the Opacity Project and thus indicating large amount absorption of radiation and higher opacity. The new results on photoionization will be illustrated and discuss on how inclusion of these will increase and provide more accurate opacities and narrow down the gap of difference between the observed and predicted opacities, and thus findings more precise elemental.

Keywords- Solar composition; plasma opacity; resonant opacity; Z-pinch experiment.

WHAT IS NEW OR PUZZLE ABOUT OUR SUN?

A recently published Nature article with the topic tiled "A higher than predicted measurement of the iron opacity at solar interior temperatures"[1] has brought much attention to astrophysics, atomic physics, plasma physics, solar physics communities. The National Public Radio (NPR) even had a press release with title "Scientists Bring the Sun Down To Earth To Learn How It Works". The Z-machine at the Sandia National Lab in New Mexico is able to create an iron plasma at the very high energy density (HED) and temperature similar to that in the convection near boundary with radiative zone of the sun. At each shot, Sandia Z-machine uses 27 Mamp, a current that is higher than the total usage of current inside USA during the shot period and is producing the most intense x-ray radiation to study the plasma opacity. For verification of the measurement, Bailey et al repeated the experiment 60 times, each costing $200,000. The article presents the latest findings and updates on the solar iron opacity. Opacity depends on the composition and abundances in the plasma.

Although studied extensively, both observationally such as by the dedicated space observatory SOHO, and theoretically such as by the international team of physicists and astrophysicists under the Opacity Project,[2] there remains longstanding discrepancies between predictions and observations in fundamental quantities. The sun is not only the energy source for the earth, it is also the standard to study other stars. The composition of the Sun, the benchmark for astronomical objects, has been a longstanding problem for the last few decades (e.g.[?]). The abundances of common elements in the sun, such as, carbon, nitrogen, oxygen, supported by helioseismology, which uses acoustic oscillations to determine the internal solar structure very accurately, are at discrepant by up to 50% higher from those derived from state-of-the-art spectroscopy and elaborate 3-D radiative transfer models (e.g.[3]). The inaccuracy in composition affects study of helioseismology, primordial helium abundance, cosmological distances derived from Cepheid period-luminosity relation, etc.

After years of effort on higher precision and repeated shots at the Z machine (e.g.[5]) scientists headed by J.E. Bailey created iron plasma at 1.92.3 MK and electron densities of $(0.74.0)\times10^{22}$ per cm^{-3} and measured the iron opacity. Iron accounts for a quarter of the total opacity in the convection zone near the boundary with radiative zone. They find that the measured opacity is much higher, 30-400 %, than the predictions, such as, calculated using the atomic data from the Opacity Project.

Along with experimental work at Sandia lab to resolve the discrepancy in opacity (e.g.[5]), theoretical investigation has also been carried out.[8,10,29] New features in the atomic process of photoionization, one main factor for opacity,

provided the definite signature of significant amount of missing photoabsorption in the currently available opacities.[8] The present report gives some details of latest findings and updates on determination of solar opacity of higher accuracy.

Plasma Opacity

Opacity is a fundamental quantity for radiation transport in a medium. Determination of opacity particularly for plasmas is highly essential as 99% of our known universe is made of plasma at various temperatures and densities. Fig. 1 illustrates physical conditions of plasmas of various regimes. The present interest is in the plasma in the region of stellar interiors. Plasma opacity is used in models of astrophysical and laboratory plasmas for determination of elemental abundances, physical conditions, stellar pulsations, internal structure, chemical composition, evolution of states, such as, in local thermodynamic equilibrium (LTE).
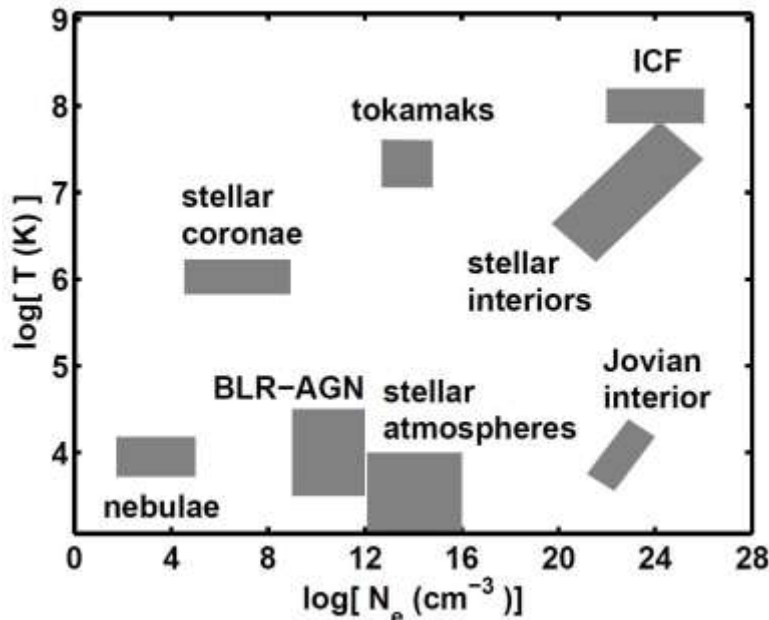

Fig. 1: Plasma covers vast region in temperature-density (T-ρ) phase space and many physical regimes[6].

As the radiation propagates through plasma, it loses energy and slows down by absorption and emission by the constituent elements. The effect of radiation absorption is described by opacity, such that high opacity means low transport and low opacity means high transport of radiation. Fig. 2 shows the radiation intensity opacity relation in a plasma. The ratio of the initial intensity, I_o and the final intensity, I, after passing through a region of depth of x is given by transmission T as

$$Transmission(T) = \frac{I(v)}{I_0(v)} = \exp(\tau) \tag{1}$$

where the optical depth τ is related to opacity κ as $\tau = \kappa(v)x$ Calculation of opacity is quite involved and extensive. It depends on the all possible radiative transitions for all ionization states of all elements exist in the medium. Accurate consideration of such large number of transitions is an enormous job.

The sun is huge ball of extremely dense and hot plasmas which vary from center to the surface. The core, where nuclear fusion takes place, temperature is about 15 MK degrees and density is 100 g/cc which is more dense any solid we know. Gamma rays generated from nuclear fusion travel outward in the radiative zone where the plasma is assumed to be uniformly dense and then in the convection zone where plasma is turbulent before escaping the sun. By this time, the large part of gamma rays has reduced to optical radiation due to
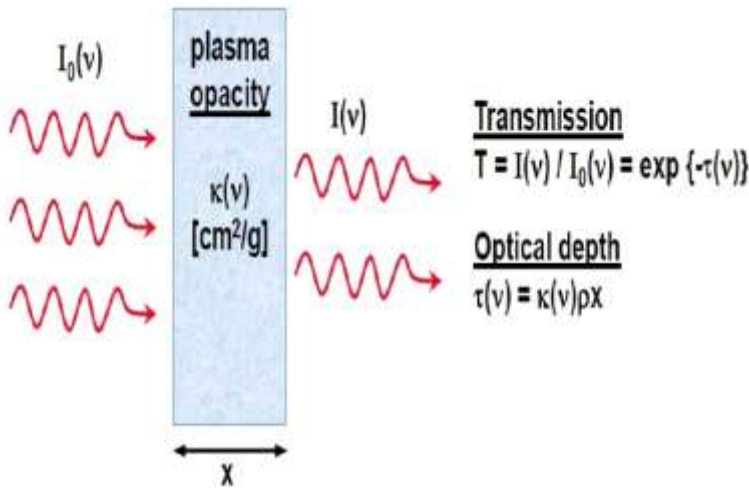
Fig. 2: Change in intensity of radiation passing through a distance of "x" in the plasma is due to the opacity.

solar plasma opacity. The boundary between the radiative and convection zones, R_c, where the plasma phase changes is well known from helioseismology or optical oscillations of the sun. The measured value is 0.713 ± 0.03 from the core. The predicted boundary, using the current opacity, has a larger value of 0.726 and has been a problem for over a decade.

Photo-excitation, photoionization and opacity

Microscopically opacity $\kappa(v)$ depends on the atomic process of photo-excitations, photoionization and photon scattering. For the photon-ion interactions, it depends on the oscillator strengths and photoionization cross sections of all possible transitions. κ_v also needs elemental abundances. Photo-excitation that absorbs a photon can be described as

$$X^{+Z} + hv \rightarrow X^{+Z*}$$
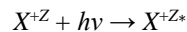
where X^{+Z} is the ion with charge Z. The strength of the photoabsorption is determined by oscillator strength (f). f_{ij} is related to $\kappa(v)$ as

$$\kappa_\nu(i \rightarrow j) = \frac{\pi e^2}{mc} N_i f_{ij} \phi_\nu \tag{2}$$

where N_i is the ion density in state i, φ_v is a profile factor which can be Gaussian, Lorentzian, or combination of both over a small wavelength range.

In photoionization, an electron is ejected with absorption of a photon,

$$X^{+Z} + h\nu \rightarrow X^{+Z+1} + \epsilon$$

In addition to direct photoionization, the process can occur via an intermediate doubly excited state as:

$$e + X^{+Z} \rightleftharpoons (X^{+Z-1})^{**} \rightleftharpoons \begin{cases} e + X^{+z} & AI \\ X^{+z-1} + hv & DR \end{cases}$$
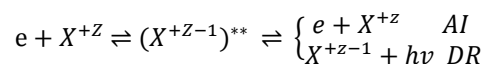
Here a colliding electron excites the target and attaches to form the short-lived doubly excited quasi-bound autoionizing state. The autoionizing state leads either to autoionization (AI) where the electron goes free and target drops down to the ground state or to dielectronic recombination (DR) where the electron gets bound by emission of a photon. The inverse of DR is photoionization. The autoionizing state manifests as an enhancement or resonance in the process and hence crucial to proper inclusion in the calculations. The probability of photoionization is determined by cross sections (σ_{PI}) which is related $\kappa(v)$ as

$$\kappa_v = N_i\,\sigma_{PI}(v) \tag{3}$$

κ_v depends also on two other processes, inverse bremsstruhlung or free-free (ff) scattering and photonelectron scattering. In inverse bremsstrahlung, a free electron and an ion can absorb a photon in free-free interaction,

$$h\nu + \left[X_1^+ + e(\epsilon)\right] \rightarrow X_2^+ + e(\epsilon'), \tag{4}$$
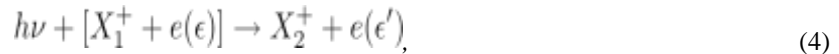
The free-free scattering cross sections can be obtained from calculation of the elastic scattering matrix elements for electron impact excitation of ions. An approximate expression for the free-free opacity is given by

$$\kappa_\nu^{ff}(1,2) = 3.7 \times 10^8 N_e N_i g_{ff} \frac{Z^2}{T^{1/2}\nu^3} \tag{5}$$

where g_{ff} is a Gaunt factor.

The photon electron scattering can be of two types, Thomson scattering, when the electron is free and Rayleigh scattering when the electron is bound to an atomic or molecular species. κ is constant for Thomson scattering and is proportional to its cross section σ^{Th},

$$\kappa_{sc} = N_e\sigma^{Th} = N_e \frac{8\pi e^4}{3m^2c^4} = 6.65 \times 10^{-25}\ cm^2/g, \tag{6}$$

κ is proportional to Rayleigh scattering cross section σ^R as

$$\kappa_\nu^R = n_i\sigma_\nu^R \approx n_i f_t\ \sigma^{Th}\left(\frac{\nu}{\nu_I}\right)^4 \tag{7}$$

where n_i is the density of the atomic or molecular species, $h\nu_I$ is the binding energy and f_t is the total oscillator strength associated with the bound electron, i.e. the sum of all possible transitions, such as the Lyman series of transitions i$s \rightarrow np$ in hydrogen.

The elemental densities or abundances can be obtained from proper equation of state (EOS) which gives the ionization fractions and level populations of each ion of an element in levels with non-negligible occupation probability. For example, for plasmas in local thermodynamic equilibrium (LTE) Saha equation is used for the EOS. However, Saha equation is not applicable in non-LTE condition. Some details of the opacity calculations can be found in.[6]

The above discussions are for monochromatic opacities κ_v. These values are used to obtain the averaged opacity, most commonly the Rosseland mean opacity, κ_R, at the plasma conditions of temperature and density. Rosseland mean opacity $\kappa_R(T,\rho)$ is the harmonic mean opacity averaged over the Planck function, $g(u)$,

$$\frac{1}{\kappa_R} = \frac{\int_0^\infty \frac{1}{\kappa_\nu}g(u)du}{\int_0^\infty g(u)du}, \tag{8}$$

where $g(u)$ is given by

$$g(u) = \frac{15}{4\pi^4}\frac{u^4 e^{-u}}{(1-e^{-u})^2}, \quad u = \frac{h\nu}{kT} \tag{9}$$

$g(u)$, for an astrophysical state is calculated with different chemical compositions of H, He, and metals, that is, all other elements starting from Li. The typical notation for abundances is X for H, Y for He and Z for metals. For any astronomical object, they are related as

$$X + Y + Z = 1 \tag{10}$$

THE OPACITY PROJECT, THE IRON PROJECT, THE IRON OPACITYPROJECT

Astrophysical opacities were incorrect by factors of 2 to 5 until efforts were made by the Opacity Project (OP) team[2] and soon after by OPAL group.[11] The exiting R-matrix method using close-coupling expansion was extended[12,13] to study the atomic processes with excited states going up to n = 10 in ab initio manner. The OP team made the first systematic and detailed study of radiative processes of photo-excitation and photoionization of all atoms and ions from hydrogen to iron that are astrophysically abundant. Large amount of atomic data for energy levels, oscillator strengths and photoionization cross sections were calculated which are available at data base TOPbase[14] at CDS. The opacities

obtained from the atomic data are available at OPserver.[15] New features in photoionization cross sections were revealed. Many long standing problems solved the pulsation ratios of Cepheid variables. Opacity structures for various levels of the sun were obtained.[16] The lowering of black body radiation curve was explained by photoabsorption by low ionization states of iron ion, such as, Fe II.[17] X-ray emission of dielectronic satellite lines of iron ions, as observed in solar storm, were reproduced.[18] OP also showed the existence of the Z-bump in the solar opacity which is dominated by iron ion as shown in Fig. 3.[16] OP data continues to solve many astrophysical problems. However, a large part of the data is not precise enough for various diagnostics and astrophysical problems. Hence calculations for new results with larger wave function expansion being carried out and available on-line at NORAD-Atomic-Data website.[19]
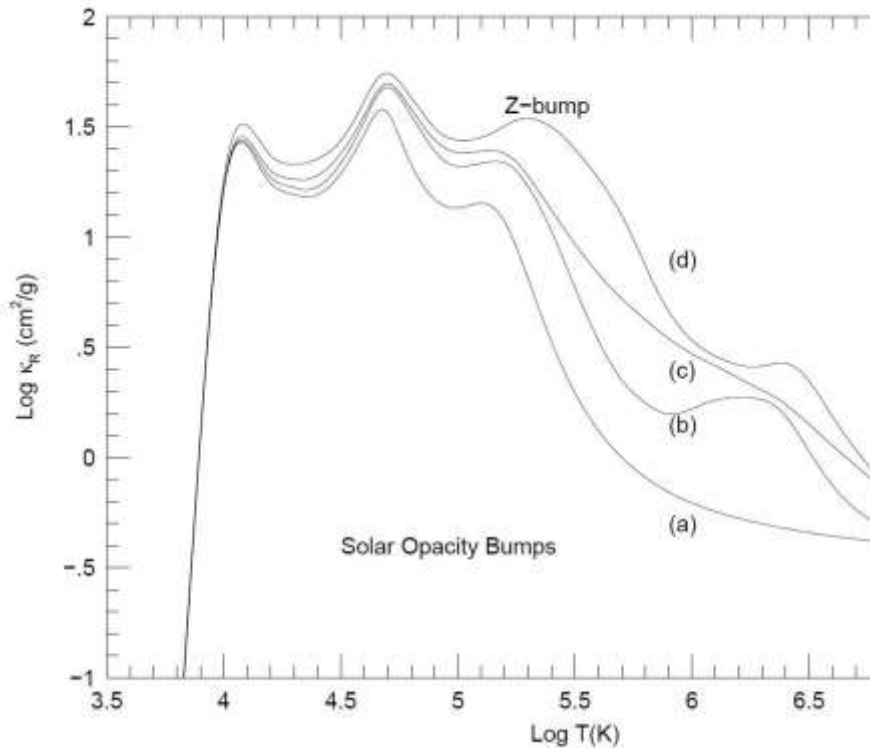

Fig. 3: Increment of Rosseland mean opacity κ_R with elements at R=-3. $\mathbf{R} = \rho(\mathbf{g/cc})/\mathbf{T_6^3}, \ \mathbf{T_6} = \mathbf{T} * \mathbf{10^{-6}}$ is related to depths in a star. Several bumps associated with excitation and or ionization of different atomic species are seen. The first (lowest κ_R) curve (a) has three bumps corresponding to the ionization of neutral H, He, and He II, at $Log \ T \approx 4$, 4.6, and 5.2 respectively. Including elements up to Ne raises the opacity towards higher temperatures as in curve (b). In addition, another bump appears at $Log \ T \approx 6 -$ 6.5 which is related to highly ionized ions. Addition of further elements up to Ca raises the overall opacity significantly as shown in curve (c). The topmost curve (d) is due to the further inclusion of the iron group elements up to Ni, that gives rise to a considerable increase in opacity for all $T > 10^4$ K. The most outstanding enhancement in opacity due to iron occurs curve (d), $Log \ T = 5.2 - 5.6$, referred to as the Z-bump. It is mainly due to excitation and ionization of Fe ions with partially filled M-shell (n = 3), Fe IX -Fe XVI.[16]

The OP was extended to the Iron Project[20] to include collisional excitations in iron-peak elements. The team extended the R-matrix codes for radiative processes[13] using nonrelativistic LS coupling approach to relativistic R-matrix method in Breit-Pauli approximation to include fine structure where the method was named as Breit-Pauli R-matrix or BPRM method.[21] New algorithm for theoretical spectroscopy has been developed for consideration of large number of fine structure levels for all practical purposes.[22,23] Details of the R-matrix calculations can be found in the OP, IP references as well as in the text book[6].

Although the sun has been one main objective to study under the OP, the computed opacities do not solve problem of elemental abundances as determined by the detailed 3D hydro NLTE model from photosphere spectral analysis.[27] One major problem is with the observed and predicted boundary between the solar radiative zone and the convection zone, R_C. The boundary is known to be accurately measured from helioseismology as 0.713 relative to the total solar

radius. R_C can be predicted from opacity through elemental abundances in the solar plasma as the optical depth is related to the opacity. The calculated boundary is found to be R_C is 0.726, a much larger value than the measured value. It was estimated that the discrepancy in abundances could be solved if opacity was increased by about 15% (e.g.[4]). To resolve the problem by obtaining accurate opacity Sandia National lab and Ohio State University jointly initiated the Iron Opacity Project. Iron ions, through their much larger number of bound levels compared to lighter ions, are capable of absorption of considerable number of photons and hence account for higher opacity. It has been verified through both observation and measurement that at the HED condition of convection zone near the boundary with radiative zone, the dominating iron ions are Fe XV - XX as seen in Fig. 4.
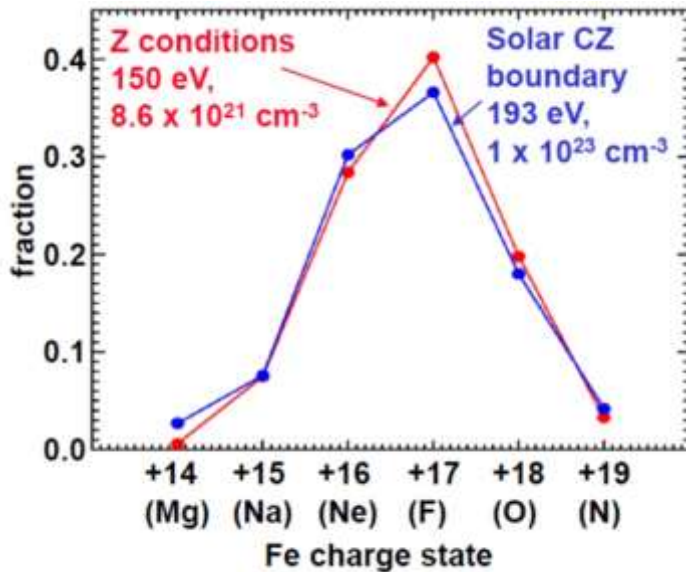

Fig. 4: Abundances of iron ions in the convection zone near the boundary with radiative zone in the sun as observed (blue) and measured (red).

Under the Iron Opacity Project, which also overlaps with the Iron Project, oscillator strengths for all dominant iron ions in the convection zone have been obtained: Fe XIV,[29] Fe XV,[26] Fe XVI,[27] Fe XVII,[24] Fe XVIII,[25] Fe XIX,[28] Fe XX.[30] Due to fine structure transitions which allows both same spin and intercombination transitions, the number of transitions for each ion has increased considerably compared to earlier OP data. The next study is for photoionization for which computations are much more extensive than that for radiative transitions or photoexcitations.

Study of photoionization cross sections of Fe XVII with a large wave function expansion using 60 core states which include highly excited n = 3 states has been reported.[7,8] As seen in Fig. 4, Fe XVII is the most abundant ion in the solar plasma in the convection zone, and hence been the focus for detailed theoretical investigation of the resonances in photoionization cross sections of the ion. Computation for photoionization cross sections of Fe XVIII with a large wave function expansion is in progress.

CREATING THE SUN ON THE EARTH AT Z-MACHINE

Concurrent to theoretical progress, Sandia National Lab (SNL) has been carrying out opacity measurement of iron plasma created at the Z-pinch machine. It creates magnetically driven implosions in plasmas to convert electrical energy into radiation through internal shock. At Sandia, an extremely high current of 27 MAmp is passed through the gold haulram which explodes creating most intense x-rays at 1.5 MJ. X-rays are passed through the iron plasma created from iron filament heated uniformly to stellar interior conditions (with temperature to about $T_e \sim 190$ eV or 2 MK and density about $n_e \sim 2.8 \times 10^{22}/cm^3$) and maintained an electron population distribution that can be described by the local thermodynamic equilibrium (LTE). Magnesium is included in the plasma for the diagnostics of temperature and density.

Fig. 5 gives of view of the opacity measurement. A spectrometer that views the back light directly and through the sample determines the spectrally resolved transmission. The opacity is determined by taking the natural log of the transmission and dividing by the areal density.
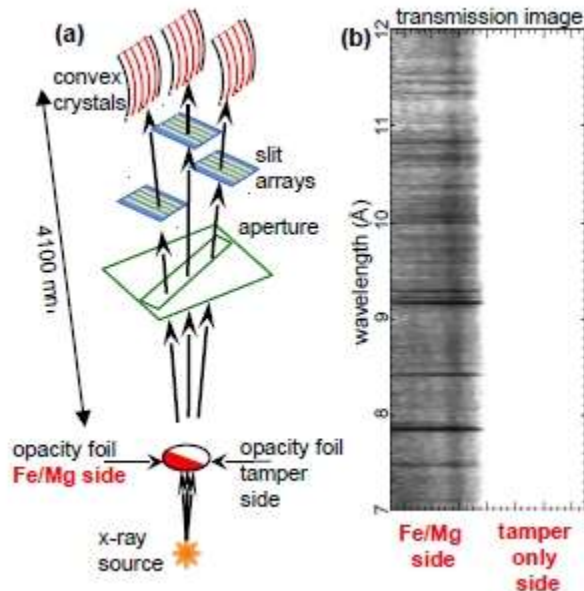

Fig. 5: Experiment. a: spectrometers view the half-moon shaped tamped iron/magnesium sample. Each spectrometer employs multiple slits to project space-resolved images onto a convex crystal that disperses the spectrum before recording on film. The setup measures the unattenuated (tamper only) and the attenuated (tamper plus FeMg) spectra on the same experiment. b: A space and spectrally-resolved transmission image is obtained by dividing the attenuated spectral image by the unattenuated image. Darker regions correspond to higher absorption. The white portion of the image corresponds to 100% transmission[1].

LATEST EXPERIMENTAL RESULTS

The high precision measurement at Sandia Z-machine studied opacity of stellar plasmas at various temperature and density, T_e/n_e. Fig. 6 presents opacities at four different T_e/n_e. The measurements combine information from 22 separate experiments The SCRAM model calculations show (blue) similarities of opacity with observed features (red) only at the lower temperature/density of plasma and become worse with higher T_e/n_e.

Iron opacity spectra at $T_e=2.11\times10^6$ K, $n_e=3.1\times10^{22}$ cm^{-3}, condition at the solar radiation/convection zone boundary, is compared with multiple models in Fig. 7. The measured opacity (black) represents an average obtained by combining information from five separate experiments with four independent spectrometers. The calculations account for the instrument resolution and the experiment error bars represent 1σ uncertainties. The top panel where the measured data (black) is compared with the OP model (cyan) shows large differences, particularly in the background. The ratio of the experiment opacity with OP and other models in the bottom panel ranges a wide differences, going from 30 - 400%. The Rosseland mean opacities (dotted black and cyan lines in the top panel) calculated in the wavelength range of 6 - 13 ˚A also indicate large difference between the OP model (with solar mixing) and that from experiment. Although OP has most accurate atomic data compared to those used by other models, no visible improved agree can be seen. These differences are assumed to be largely from incomplete data, approximations in the equation of state (EQS) for level populations, and missing physics of the physical process of resonant absorption in the high energy region which will be illustrated in the section below.

NEW THEORETICAL FINDINGS AT ENERGY PHOTOIONIZATION

In the observed opacity spectra,[1] most of the resonant structures arise from bound-bound transitions which can be verified by the energy positions. The background, which is found to be enhanced, is contributed by photoionization cross sections. Opacity due to photoionization is caused mainly by photons absorption through quasi-bound resonances. These resonances arise from excitations of the core in combination with another loosely temporarily bound

electron. The resonant structures in photoionization may not show sharp features like pure bound-bound transitions because of averaging by the temperature, density mapping, but they are the main contributor to the background opacity.
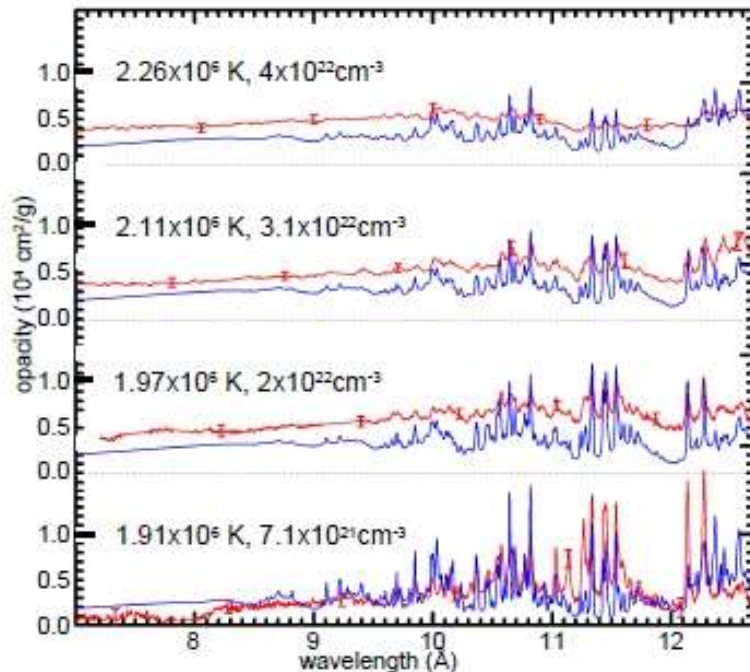

Fig. 6: Measured iron opacity spectra (red) at four $T_e e/n_e e$ values are compared with predicated values (blue) calculated using the SCRAM model which accounts for the instrument resolution. With higher temperature and density, the measured opacity becomes more featureless while the background shows larger difference with the predictions[1].

The OP work considered the resonances in photoionzation of many bound states of an atomic system for the first time (e.g.[14]). However, the work included only the low energy resonances. The reason was the assumption that most of the dominant couplings of channels lie with the lower excitations of the core ion, particularly with states in the same complex, Δn=0. Computational capability of the available computers, although not the top, was also an issue. However, later investigations revealed that high lying core excitations also play very important role in introducing extensive and high peak resonances.[31] Inclusion of relativistic fine structure effects revealed resonances at low energy not allowed in LS coupling approximation. These structures, not studied before, can be very important for low temperature plasmas (e.g.[32]).

Using a 60 level or 60 CC calculations for photoionization cross sections of Fe XVII, Nahar group[7,8] found extensive and strong resonances that belong to n=3 core levels in the high energy regions compared to those belong to n=2 levels. It was unexpected since the energy gap between the two complexes n=2 and 3 is about 47 Ryd for which couplings of channels are expected to be minimum. They explained the findings as missing opacities in the present OP models since these newly found resonances correspond to considerable amount of photoabsorption and will increase opacity (e.g.[10]). Nahar et al.[8] obtained cross sections of 454 bound levels with n ≤ 10. They calculated, using the new atomic data for oscillator strengths[24] and photoionization cross sections,[8] monochromatic opacity κ for Fe XVII at temperature T = 2.24 ×10^6 K, electron density $n_e = 10^{23}$ cm^{-3}, similar to that near the solar convection-radiative zone boundary. Comparison of new κ Fig. 8 (top panel) with that available at Opacity Project server OPserver[15] Fig.8 (bottom panel) shows considerable enhancement in the new opacity for Fe XVII not seen earlier (Fig.8, bottom). Although similarities between the two opacity curves can be seen, there are differences in the atomic data. The OP curve included atomic data from 2-CC wave function expansion with addition of resonances of high core-excitations as lines where autoionization widths are considered perturbatively, and high-energy K-shell continuum opacity not yet included in 60-level BPRM calculations. Integration of the new opacity for the Rosseland mean opacity found an increment of opacity by 20% over the OP opacity. The new results were not included in the Sandia Z opacity comparison with predicted opacity because of incomplete data for the set of iron ions. Bailey et al.[1] comparison

includes data available at TOP base. Regardless of direct comparison, the new findings in Fe XVII opacity confirms enhancement in the measured opacity spectra at Sandia Z-machine.
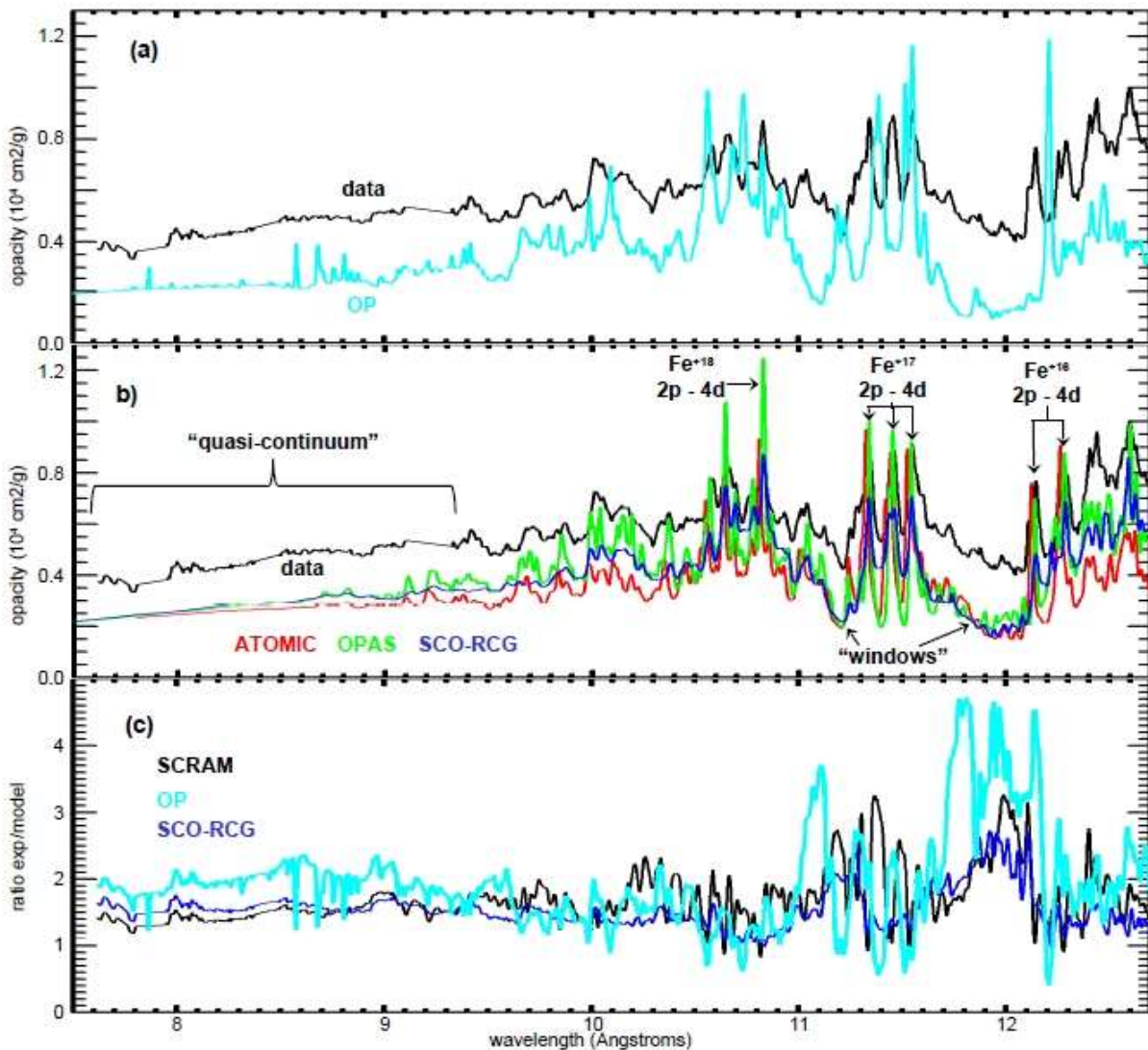

Fig. 7: Comparisons of observed iron opacity spectra (black curve) with multiple models. OP (cyan, at top and bottom panels), SCO-RCG (blue), ATOMIC (red), OPAS (light green) at the solar convection zone boundary temperature and density: $T_e = 2.11$MK, $n_e = 3.1 \times 10^{22}$ cm^{-3}. a. OP model uses for solar modeling. The dashed lines are the Rosseland mean opacities calculated for this wavelength range. b. Comparisons with three other models. c, Ratio of the experiment opacity with three different models.[1] Considerable differences can be seen between the measured and predicted opacities.

In order to find the importance of contributions from high lying excited states, higher than the 60-level calculations, a new work is in progress to calculate photoionization cross sections of Fe XVII using a 99-CC wave function expansion in LS coupling which correspond to 218 levels in fine structure. Since fine structure BPRM calculations are several times larger than LS coupling calculations, present study considers LS coupling to enlarge the energy range and see the impact in the high energy. The 99-CC wave function expansion includes additional n=3 LS states (not included in 60-CC fine structure level expansion) and n=4 states. A comparison of cross sections of the present and previous 60-CC and OP 2-CC calculations is given in Fig. 9. Comparison shows very clearly that the opacity from the OP model which uses data, such as that of panel (c),[14] has considerable amount of photoabsorption missing, will give grossly underestimated opacity.

CONCLUSION

This report presents the new findings on solar opacities and current status of efforts toward narrowing down the differences between prediction and observation and a clear understanding of the opacity and abundances of elements in the sun.
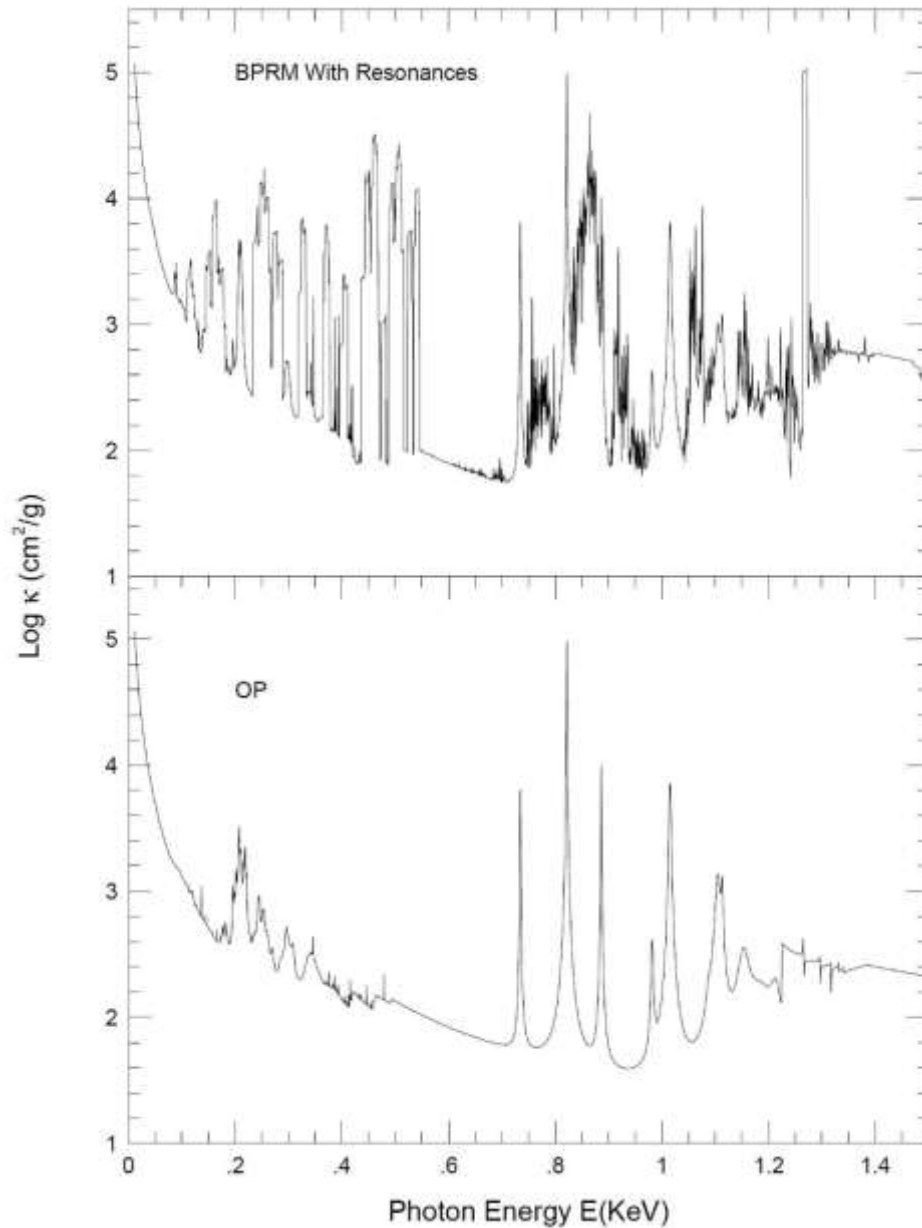

Fig. 8: Monochromatic opacity of Fe XVII at temperature T = 2.24 ×10^6 K and electron density N_e = 10^{23} cm^{-3}, corresponding to the base of the solar convection zone. The top panel presents opacity obtained using new atomic data from 60 CC wave function expansion and the bottom panel the total OP opacities which uses TOPbase data.[14] OP model includes resonances of high coreexcitations, which are not included in the wave function expansion, as lines which are broadened with autoionization widths perturbatively, and the high-energy K-shell continuum opacity not yet included in 60-CC calculations[8].
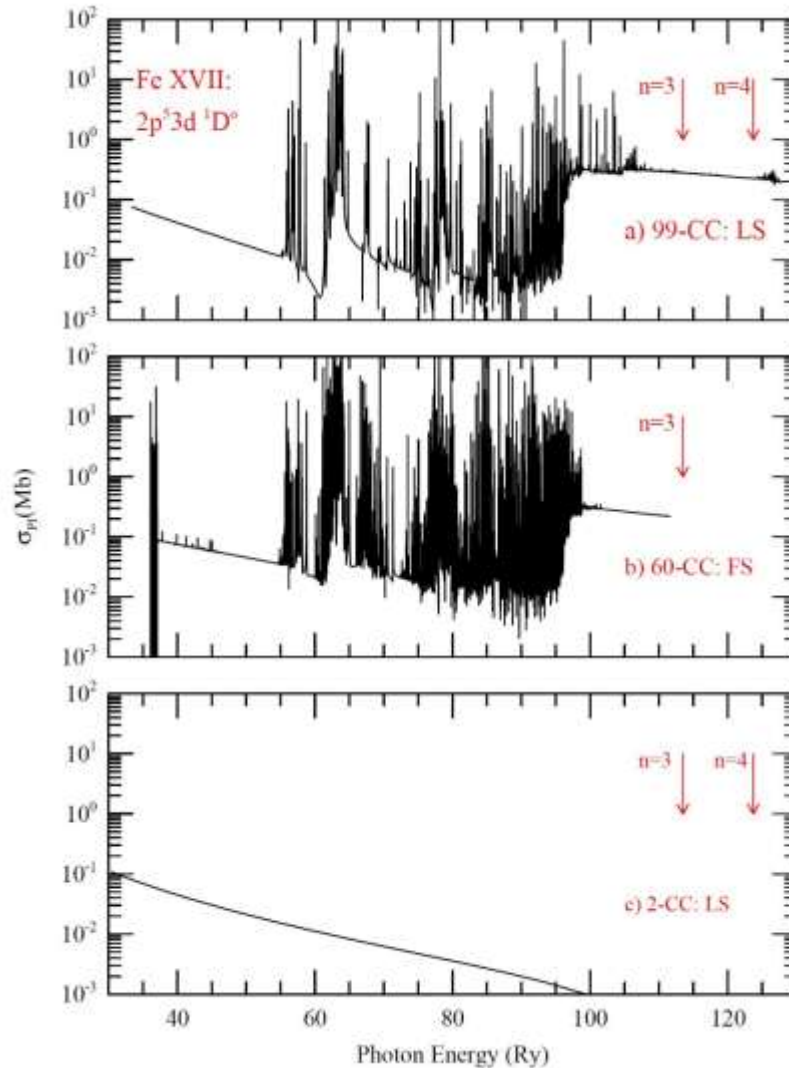
Fig. 9: Photoionization cross sections σ_{PI} of $2s^2 2p^5 3d(^1D^o)$ state of Fe XVII in the R-matrix calculations: a) present 99-CC expansion in LS coupling, b) 60-CC expansion in fine structure (FS),[8] c) 2-CC expansion in LS coupling under the OP.[14] The arrows indicate energy positions for the last n=3 and n=4 core excitations. σ_{PI} in FS (b) has more resonances due to couplings of more channels and finer energy mesh and in 99-CC LS (c) has additional resonances, although not very strong, and a very slow decaying background.

ACKNOWLEDGMENT

REFERENCES

1. J.E. Bailey, T. Nagayama, G.P. Loisel, G.A. Rochau, C. Blancard, J. Colgan, Ph. Cosse, G. Faussurier, C.J. Fontes,F. Gilleron, I. Golovkin, S.B. Hansen, C.A. Iglesias, D.P. Kilcrease, J.J. MacFarlane, R.C. Mancini, S.N. Nahar, C.
    Orban, J.-C. Pain, A.K. Pradhan, M. Sherrill, B.G. Wilson, *Letter, Nature* **517**, 56 (2015)

2. The Opacity Project Team.*The Opacity Project*, Vol 1 (1995), Vol. 2 (1996) (Institute of Physics Publishing)

3. M. Asplund, N. Grevesse, J.A. Sauval, P. Scott, *Annu. Rev. Astron. Astrophys.* **47**, 481 (2009)

4. J.N. Bahcall et al. *Astrophys. J.* **614**, 464 (2004)

5. J.E. Bailey et al. (22 authors), *51st Annual meeting of the Division of Plasma Physics (DPP) of APS*, Atlanta, Georgia, November 2-6, 2009, TOc.010

6. *Atomic Astrophysics and Spectroscopy*, A.K. Pradhan and S.N. Nahar (Cambridge University Press, 2011)

7. H.Lin Zhang, S.N. Nahar, and A.K. Pradhan, *Phys. Rev. A* **64**, 032719 (2001)

8. S.N. Nahar, A.K. Pradhan, G.X. Chen, W. Eissner, *Phys. Rev. A* **83**, 053417 (2011)

9. S.N. Nahar, Proceedings of the 4th international conference on MTPR-10, *Modern Trends in Physics Research*, Sharm El Sheikh, Egypt, December 12-16, 2010 (Editor: Lotfia El Nadi, World Scientific, 2013), p.15-28

10. S.N. Nahar, *Can. J. Phys.* **89**, 439 (2011)

11. C.A. Iglesias and F.J. Rogers, *Astrophys. J* **371**, 40 (1991)

12. M.J. Seaton, *J. Phys.* B **20**, 6363 (1987)

13. K.A. Berrington *al. J. Phys.* B **20**, 6379 (1987)

14. TOPbase: http://cdsweb.u-strasbg.fr/topbase/topbase.html

15. OPserver: http://opacities.osc.edu/

16. M. J. Seaton *et al.*, *Mon. Not. R. Astron. Soc.* **266**, 805 (1994)

17. S.N. Nahar and A.K. Pradhan *J. Phys. B* **27**, 429 (1994)

18. S.N. Nahar, A.K. Pradhan, *Phys. Rev. A* **73**, 062718 (2006)

19. NORAD-Atomic-Data: www.astronomy.ohio-state.edu/∼nahar/nahar radiativeatomicdata/index.html

20. D.G. Hummer *et al. Astron. Astrophys* **279**, 298 (1993)

21. K.A. Berrington *et al. Comput. Phys. Commun.* **92**, 290 (1995)

22. S.N. Nahar, A.K. Pradhan, *Phys. Scr.* **61**, 675 (2000)

23. S.N. Nahar, *Astron. Astrophys. Suppl. Ser.* **127**, 253 (2000)

24. S.N. Nahar, W. Eissner, G.X. Chen, A.K. Pradhan, *Astron. and Astrophys.* **408**, 789 (2003)

25. S.N. Nahar, *Astron. Astrophys.* **457**, 721 (2006)

26. S.N. Nahar, *At. Data Nucl. Data Tables* **95**, 577 (2009)

27. S.N. Nahar, W. Eissner, C. Sur, A.K. Pradhan, *Phys. Scr.* **79**, 035401 (2009)

28. S.N. Nahar, *At. Data Nucl. Data Tables* **97**, 403 (2011)

29. S.N. Nahar, *New Ast.* **21**, 8 (2013)

30. S.N. Nahar, *Astron. Astrophys.* **413**, 779 (2003)

31. S.N. Nahar, *Astrophys. J. Suppl.* **101**, 423 (1995)

32. S.N. Nahar, *Phys. Rev. A* **65**, 052702 (2002)